MLM--3706(OP)

DE92 002031

QUANTITATIVE NONDESTRUCTIVE DENSITY DETERMINATIONS OF VERY LOW-DENSITY CARBON FOAMS

W. E. Moddeman, D. P. Kramer, D. W. Firsich, P. D. Trainer, P. S. Back, S. D. Smith, W. R. Deal, R. F. Salerno, and F. A. Koehler
EG&G Mound Applied Technologies+
Miamisburg, OH 45343

M. E. Hughes and R. N. Yancey
Advanced Research & Applications Corporation,
Wright-Patterson Air Force Base, Dayton, OH 45433

ABSTRACT

The carbon density and the carbon distribution in low-density foams that were manufactured by a modified salt-replica process were determined by bulk measurements of weight and volume and by x-ray computed tomography (CT). When determining the carbon density, both methods yielded similar results, however, the high spatial resolution of CT was found to yield nondestructive quantitative information on the carbon distribution that was not available from bulk measurements. The highest and lowest foam densities were found to occur at the edges and the interior, respectively. The carbon density at the edge was found to be a few percent up to 20 percent higher than the average foam density. The percentage of carbon buildup at the edge was determined to be inversely proportional to the foam density, and in addition, the gradient compared favorably with calculations from Fick's second law of diffusion. A calculated diffusion coefficient was interpreted in terms of foam manufacturing in the modified salt-replica process.

+Mound is operated by EG&G Mound Applied Technologies, Inc. for U.S. Department of Energy under Contract No. DE-AC04-88DP43495.

INTRODUCTION

Carbon foams have been manufactured at EG&G Mound Applied Technologies through the use of a salt replica process [1,2] that has been modified by a Mound propriety process [3]. Applications of these foams have been described in an early publication [4]. In the basic process [1,2] of manufacturing the foams, salt is pressed into bars; the bars are then cured, infused with polymer and cured again. The salt is then removed by copious solvent rinsings and finally carbonized into very porous and light-weight, briquette-like material [2,5]. In this paper, the carbon density and the carbon distribution in various foams were determined either by bulk measurements of weight and volume or by x-ray computed tomography (CT).

EXPERIMENTAL

All of the carbon foams examined in this study were made by a proprietry salt replica process developed at Mound [3]. The resulting product contains < 1000 ppm inorganic contamination and < 100 ppm residual organic material [5].

The CT studies were performed at the Wright-Patterson Research Development Center in the Materials Laboratory X-ray Computed Tomography Facility located at Wright-Patterson Air Force Base, OH. The instrument used in this study [5] was manufactured by Advanced Research & Applications Corporation (ARACOR), Sunnyvale, CA. This CT instrument operates with a 420 kV bremsstrahlung x-ray source and has a spatial resolution of ~0.25 mm. Because of the low-density of these carbon foams, the x-ray source was not filtered and the detectors used only a 1.5 mm thick aluminum filter. The instrument has two sets of detectors for each line of sight, a thin front detector to monitor low-energy x-ray attenuation and a thick back one to monitor the higher energy x-ray attenuation. This study used the front detector and utilized a detector preamplifier setting which assumed low x-ray attenuation throughout the material. This allowed for accumulation of CT data with high signal to noise ratios while still operating at the 420 kV level with the x-ray source. Several CT slices, perpendicular to all three axes, were recorded on each of the carbon foams. The carbon density was determined for each slice, and the average density of the slices and the associated standard deviation were calculated for each foam.

RESULTS AND DISCUSSION

A typical foam (a) and the accompanying cell structure (b) of the carbon product from the replica process are illustrated in Figure 1. The typical dimensions of a foam are ~10 x 20 x 100 mm. The cell structure replicates the original morphology of the salt particles; then, when the salt is removed, a cell diameter of ~5 microns is produced.

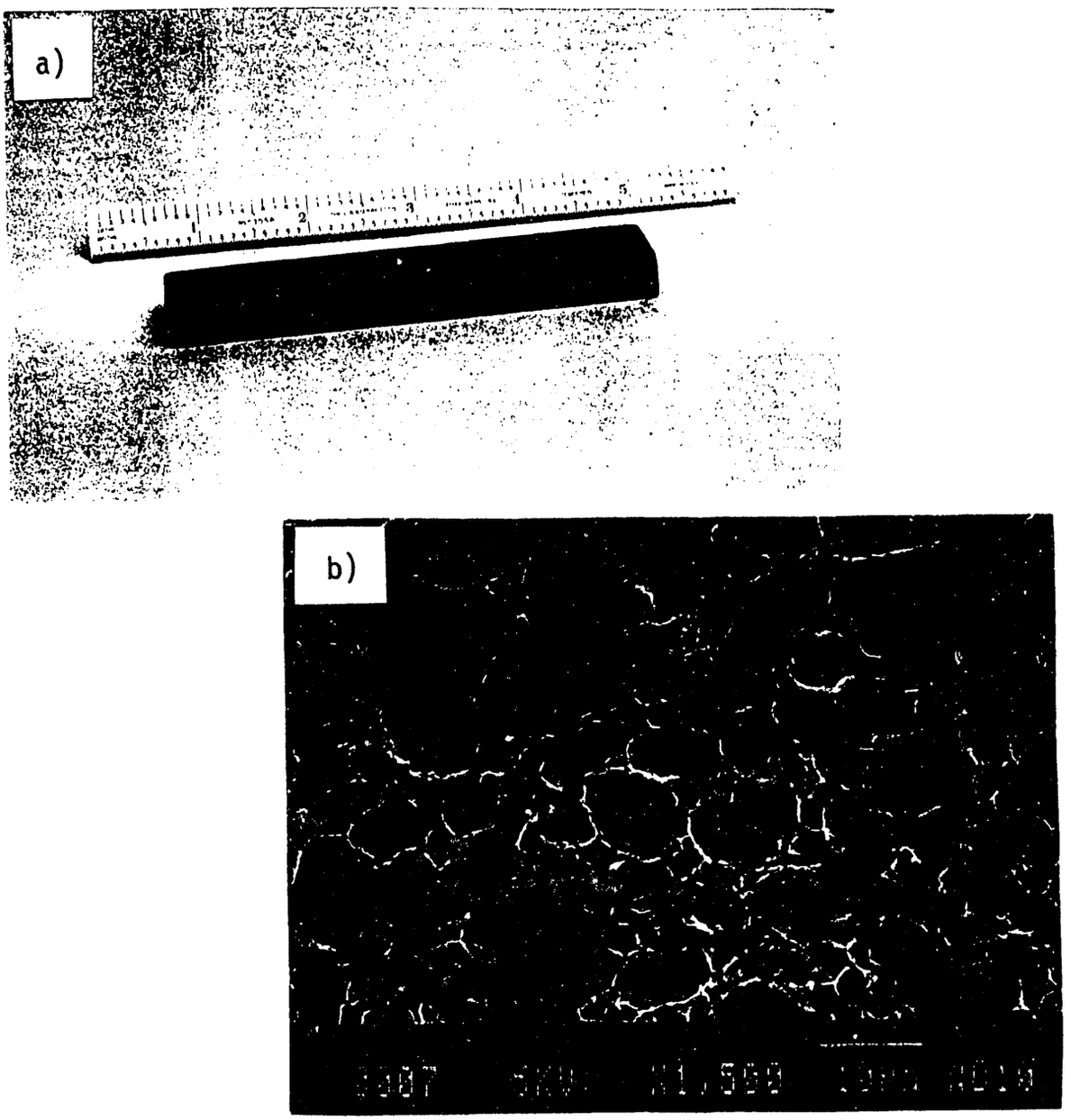

Figure 1. a) Optical and b) SEM Photographs Showing Typical Foam and Cell Structure.

The cell walls are extremely thin, often less than 0.1 microns. The density of the foams can easily be varied and have routinely been made between 29 and 60 mg/cm^3. The different densities are achieved by infusing more or less polymer into a salt bar [1-3].

The bulk density of 25 different foams were determined simply by dividing each foam weight by its volume. In addition, the density of these foams were determined by x-ray CT. As mentioned in the experimental section, the CT density for each foam is an average of several tomographic slices. The average density was calculated from a minimum of 11 determinations. These data are summarized in Table I and a plot between bulk and CT densities is presented in Figure 2.

Table I

Summary of CT and Bulk Densities
(Data in Parenthesis is Standard Deviation)

Bulk Density (mg/cm^3)	# OF CT Slices	CT Density (mg/cm^3)
29.5	11	28.92 (1.44)
33.1	11	31.70 (1.25)
35.1	11	34.32 (1.31)
35.9	11	35.59 (1.26)
36.4	11	38.03 (1.34)
37.2	11	30.84 (1.22)
40.1	11	39.54 (1.41)
40.5	11	31.53 (1.08)
42.0	11	40.81 (1.56)
43.1	11	42.28 (1.42)
43.3	15	40.46 (1.32)
43.7	15	45.23 (1.45)
44.2	15	45.38 (1.52)
44.7	15	39.97 (1.50)
45.5	15	43.36 (1.39)
45.9	15	43.40 (1.34)
46.1	15	44.57 (1.43)
46.3	15	44.42 (1.62)
46.3	15	45.49 (2.01)
50.0	11	52.90 (2.01)
50.6	15	52.55 (1.51)
51.7	11	51.15 (2.37)
55.1	15	58.29 (2.27)
56.7	11	60.29 (2.11)
59.5	11	59.85 (2.08)

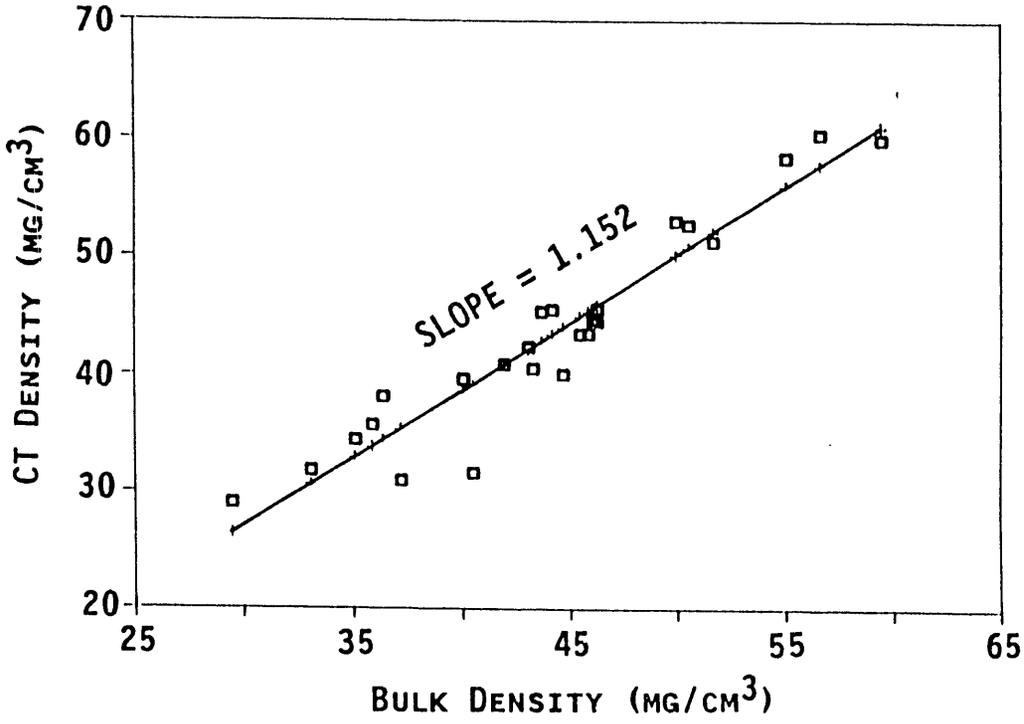

Figure 2. X-ray CT Density Plotted Against Bulk Density Showing Strong Correlation (R^2 = 0.911)

A linear regression analysis was applied to the data (Figure 2); a correlation equation was found to be:

$$\text{CT density} = -7.550 + (1.152 * \text{bulk density}) \qquad \text{eq(1)}$$

A strong correlation coefficient (R^2) of 0.911 was determined. The CT carbon data is a spatial measurement of the linear x-ray attenuation coefficient. This coefficient is a function of Compton scattering and photoelectric absorption. For carbon at 420 kV, the Compton effect clearly dominates. Since the magnitude of Compton scattering is directly proportional to the density of the electrons in a material, the CT data is expected to correlate well, and of course does, with the measured bulk density of the carbon foams.

From the data in Table I, it can be seen that, in general, the standard deviation calculated from the CT determinations increases as the bulk density increases. This can be attributed to the increased density at the edge of a foam when compared to its interior. For example, a CT slice taken at the edge of a sample is slightly higher in density than a slice that goes through the center of a foam. Figure 3 illustrates five such slices from a representative foam with a bulk density of 40.1 mg/cm^3. The data show that slices taken on the edges of a foam, (a) and (e), have a greater average density than a middle slice (c). These results are typical of all foams that are manufactured with a polymer infusion step.

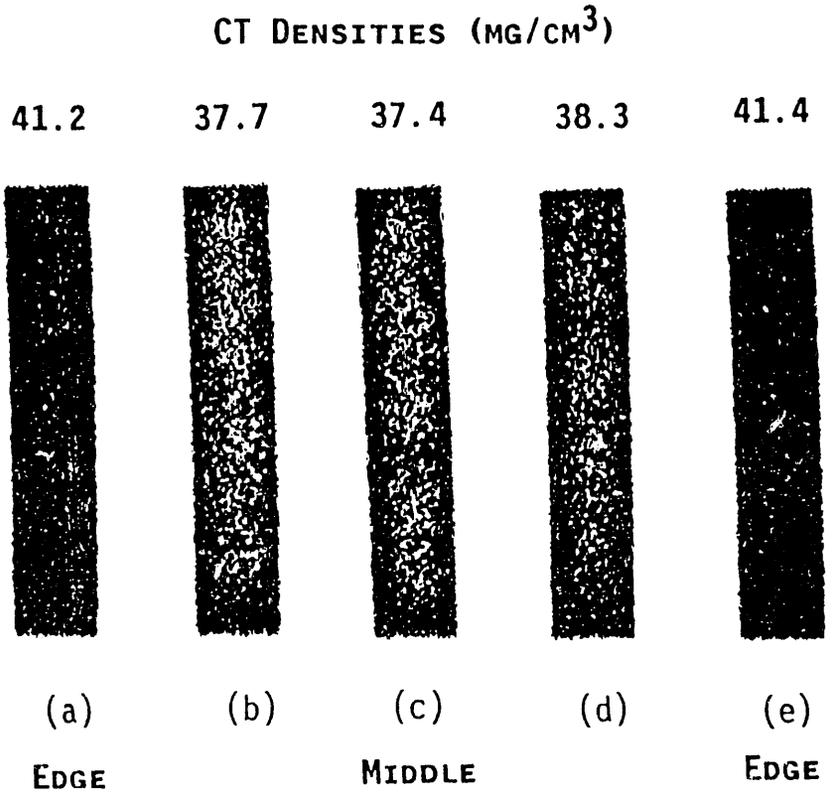

Figure 3. Five X-ray CT Slices Showing a Higher Carbon Density at Edge, (a) and (e), When Compared to Middle of Foam. Bulk Density = 40.1 mg/cm^3.

In the manufacturing of foams, salt bars are infused with polymer by submerging in an phenol-formaldehyde/acetone solution for a minimum of 24 hours [1-3]. The desired final carbon density is achieved by adjusting the concentration of the phenol-formaldehyde polymer in the acetone solution, higher densities requiring more concentrated solutions. The acetone is then removed by convection drying at an elivated temperature for a few hours resulting in an increased amount of polymer in the salt bar. After this operation, the polymer in the salt bar is set by curing; the salt is removed by several solvent leachings; and finally the porous, cured polymer is carbonized [1,2]. It is after this final step that the effect of polymer enrichment near the surface is noted.

This enrichment suggests that a diffusion process could be controlling the carbon buildup on the edges. The spatial resolution of the x-ray CT was used to measure a possible density variation that could exist within each CT slice. Data analysis was performed as illustrated in Figure 4 where the density was determined for each 'layer' within a slice. A threshold CT density was set to establish the border of all slices. This was to assure that CT data at the border, i.e. at the air/foam interface, were rejected. An erosion filter was then applied to the data. Step size of 0.58 mm was used. A 'layer' density was calculated by taking the average of the CT pixel measurements within each layer. A total of 13 layer densities were determined for each slice within a foam. These values provide information to test if a density gradient from the edge to the middle or interior of a foam is present.

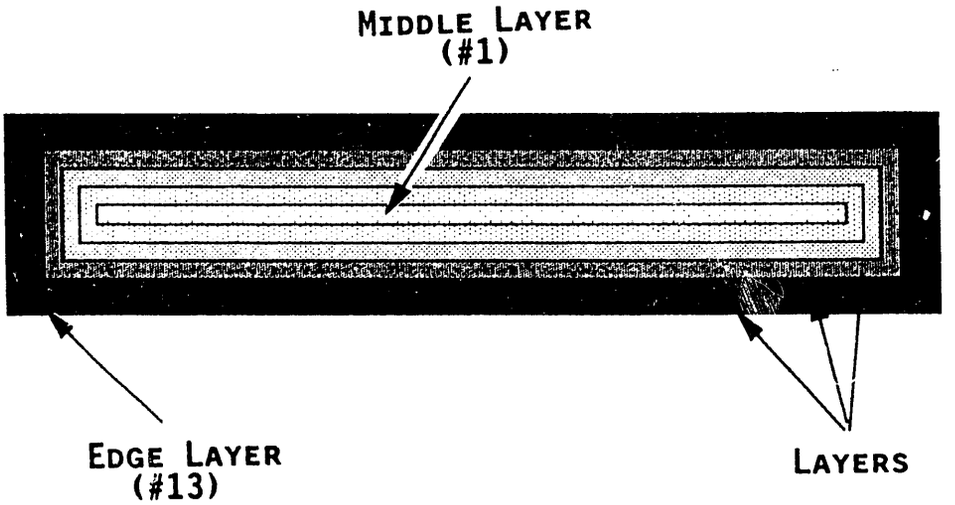

Figure 4. Schematic of Data Analysis to Obtain Average CT Density Values for Each 'Layer'.

Applying Fick's second law of diffusion to the calculated CT 'layer' densities results in the plots that are shown in Figure 5. Assuming the diffusion coefficient to be independent of polymer concentration, the data in each foam can be fitted to an exponential expression of:

$$\ln(\text{CT density}) = K + ((4)(D)(t))^{-1} x^2 \qquad \text{eq (2)}$$

where 'D' is the coefficient (cm^2/s) relatable to the diffusion of the phenol-formaldehyde/acetone solution and 't' is the time in seconds allowed for the diffusion. A strong correlation was found between CT densities and the square of the distance from the center (x^2) of three foams. Straight lines slopes of 0.264, 0.354 and 0.515 cm^{-2} were measured for foams of the following respective bulk densities of 56.7, 46.3 and 29.5 mg/cm^3. Statistical analyses on these data revealed strong regressor coefficients (R^2) of 0.965, 0.990 and 0.986. In addition to showing a strong correlation between density and square of the diffusion distance, the data reveal a inverse relationship between density and diffusion (slope in Figure 5); the greater the final density of a foam the less the diffusion of polymer.

Since diffusion occurs during the drying step, 'D' values of ~ 2.5×10^{-5} cm^2/s can be estimated from equation (2). Diffusion coefficients of this magnitude have been noted for other species dissolved in acetone [6]. For a coefficient of this magnitude, the average distance travelled by the phenol-formaldehyde/acetone solution at 60 ^{o}C during solvent removal would be ~1 cm. This is a very reasonable value based on the fact that the gradients are observed over this distance.

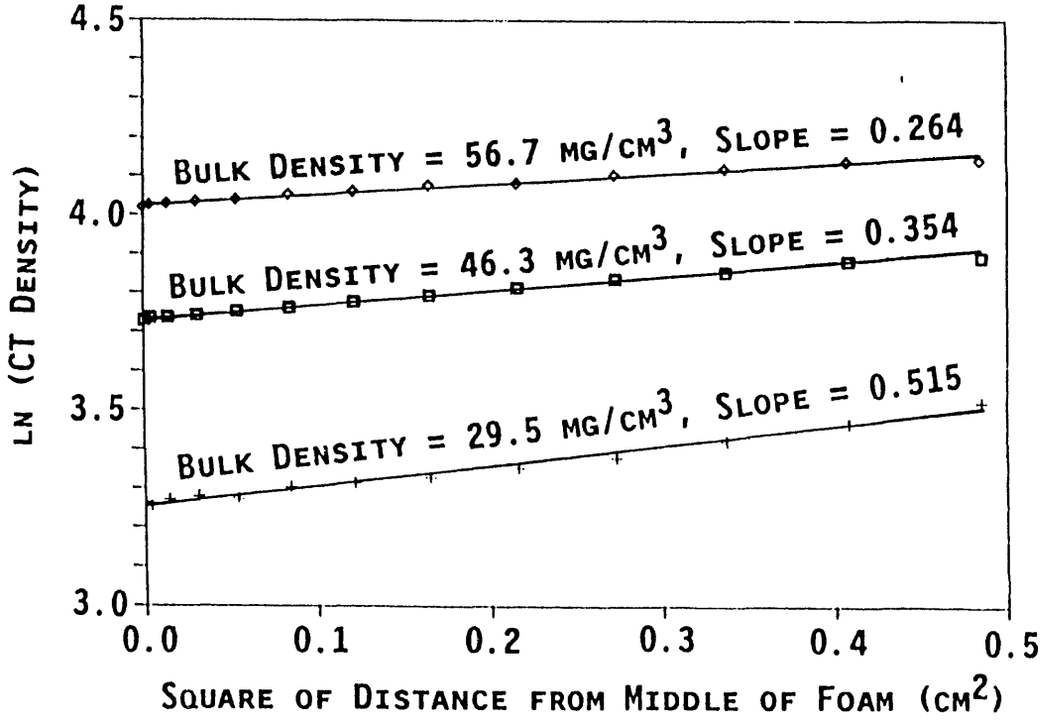

Figure 5. Carbon Density Gradient Observed on Carbon Foams.

CONCLUSIONS

The bulk densities (weight/volume) of 25 foams were compared to the densities determined by x-ray computed tomography (CT); a strong positive correlation (R^2) was found. A correlation equation of: density CT = -7.550 + (1.152 * bulk density) was established. All foams were manufactured with a polymer infusion step. Nonuniform carbon densities were observed in the high resolution CT slices of these foams. The density in these foams was found higher at the edges when compared to the interior. The CT data were fitted to Fick's second law of diffusion. This gradient was determined to be inversely proportional to the carbon density, i.e. the higher the carbon density the less the difference in between the interior and the edges. The higher carbon edge densities appear to be the result of acetone solvent drying in the foam manufacturing process.

REFERENCES

1. R. W. Hopper and R. W. Pekala, U. S. Patent Nos. 4756898, July 12, 1988 and 4806290, February 21, 1989.
2. R. W. Pekala and R. W. Hopper, J. Materials Sci., 22, 1840 (1987).
3. EG&G Mound Applied Technologies Developed Process, Miamisburg, OH. For more information contact R. F. Salerno.
4. D. A. Wrobleski, K. H. Abel, A. J. Gray and J. M. Williams, "Potential Foams and Metal Foil For Cosmic Dust Capture", Report No. LA-11271-MS, Los Alamos National Laboratory, NM, July, 1988.
5. W. E. Moddeman, D. P. Kramer, R. N. Yancey, D. L. Weirup, C. L. Logan, A. E. Pontau, A. J. Antolak and D. H. Morse, "Characterization of Low Density Carbon Foams with X-Ray Computed Tomography (CT) and Ion Microtomography (IMT)," Advanced Tomographic Imaging Methods for the Analysis of Materials, Editors: J. L. Ackerman and W. Ellingson, Materials Research Society Publication, 217, 205 (1991).
6. B. C. H. Warren and R. E. Pattle, J. Appl. Chem. Biotechnol., 27, 533 (1977).

DISCLAIMER

END

DATE FILMED

12/10/91